3D MICROCRACKING NETWORKS OF STITCHED MULTIAXIAL LAMINATES UNDER THERMAL LOADINGS

Q. Nguyen Thi Thuy, F. Valdivieso, A. Vautrin
LCG, École Nationale Supérieure des Mines de Saint-Étienne
158, cours Fauriel, F-42023 Saint-Étienne Cedex2
Email : nguyen@emse.fr

Keywords: *Stitched laminates, Microcracking, X-ray Microtomography, Thermal fatigue*

1. Introduction

Until recently, structural composites used in the aeronautical industry were still manufactured by the traditional process based on prepregs autoclaving. But occurrence of stitched multiaxial laminates NCF (Non Crimp Fabric) conducts to a new type of high performance preforms for manufacturing complex composite structures by RTM (Resin Transfer Moulding) or infusion process. However, they have a particular morphology as well as a spatial heterogeneity with resin-rich regions inside the material. In this study, a specific 3D cracking network was found out within the resin regions after the material has been subjected to thermal fatigue. The aim of this work is to focus the resin-rich regions due to stitching yarn section, which are the cause of the specific crack network under thermal cyclical loading, and not the resin-fibre heterogeneity at general composite micro-scale. In order to characterise the microcracking and determine the effect of resin-rich regions on crack initiation and propagation, a cyclical thermal loading is defined and is applied. A refined analysis relying on X-ray microtomography is carried out on test specimens, periodically.

2. Materials

The material studied is a family of composites reinforced by NC2® (Non Crimp New Concept), which is a special type of graphite fiber quadriaxial $[135/0/45/90]_S$ NCF multiaxial laminates manufactured by HEXCEL Company [9]. This laminate is composed of two unidirectional layers that consists of Toho Tenax 12K HTS 5631 fiber and HexFlow® RTM6 resin; each one has its own stitching yarn system, namely PET 76 dTex, which binds four 0.25 mm thick and 268g/m^2 plies together. Constituent properties are detailed in the Tab. 1. The only aim of using stitching yarn is to make easier the implementation and to handle the layers. The effects due to fiber disturbance are still complex to be controlled [9,10,11,12]. This leads to the concentrated areas of resin not only at the stitching holes but also in the inter-layers. The material is then a repeatedly heterogeneous structure due to the stitching location. The pattern is reproduced along longitudinal and transversal direction every 5 mm. Since each layer has its own stitching system, the material does not have a perfectly symmetric morphology [9]. More details will be showed in paragraph 4.

3. Methods

3.1 Loading conditions

The hygrothermal effect is an important parameter in aeronautics since the composite material is designed to operate under different environmental conditions. The supposed lifetime of European Supersonic Civil Transport aircraft corresponds to about 20 000 thermal cycles between -55°C and 120°C with a total length of the plateau at 120°C of 80 000 h (10 years) [13]. There is then a need of accelerated aging cycles in order to estimate the durability of materials in laboratory tests. To identify the parameters which control the mircrocracking of the material [1,2], 400 pure thermal fatigue cycles [Fig. 1] have been applied throughout this study [9]. The range of temperatures goes from -55°C up to 80°C. The dry air injection is maintained to achieve the zero humidity during conditioning.

3.2 X-ray tomography

The main reasons that makes X-ray tomography a real need for characterization of certain composite microstructures are explained clearly in the literature [3-7], the principle of the method is presented in details as well [3-8].
Throughout this non-destructive testing, the X-ray monochromatic beam is sent on a sample and the transmitted beam is recorded on a CCD detector of about 2284 pixel × 2176 pixel. The resulting image is a superimposed information (projection) of a volume in a 2D plane and the reconstructed volume is obtained with 3000 2D-images by rotating the

sample every 0.12° between 0° and 360°. The perceptibility of an anomaly part in the object depends on 3 factors: enlargement coefficient, image resolution and contrast. The achievable resolution (image sharpness) is at first influenced by X-ray source dimension. It reached the tubes filled with Nanofocus^{TM} technology values below 1 micron. The contrast is due to different absorption behaviors in different areas of a given sample. The factors affecting the absorption differences are changes in thickness or material properties and energy in this case of monochromatic source. In this study, the phase contrast mode [3] was employed because of the low density difference between the polymer resin (1.14g/cm^3) and graphite fiber (1.76g/cm^3), atomic numbers as well as in the absorption coefficients of cracks and resin [3,4,6]. A tension of about 80 kV and an intensity of about 40 mA are required in order to have a better gray level histogram with a good distinction of peak corresponding to cracks, resin and composite. A spatial resolution of 2.57 µm is obtained with a compromise between the resolution and the specimen size. The specimen dimensions are about 5.5 mm × 6.5 mm × 2 mm, that can cover the material «REV (Representative Elementary Volume)» (5 mm × 5 mm × 2 mm).

4. Results and discussion

4.1 Material morphology

After 400 thermal fatigue cycles, special specimens were cut out from the tested material to be observed. The complexity of the material morphology characterized by X-ray microtomography is shown in Figure 2.a. The resin-rich regions with cracks, the stitching yarn's filaments were also visualized in 3D direction [Fig. 3]. By using threshold segmentation, the spatial resin-rich regions were extracted, Figure 2.b shows transverse channels formed inside the plies and large interlayer gap between layers due to the stitching yarn section. All these resin-rich regions constitute a continuous resin network where cracks are found lying within.

4.2. 3D microcracking network

A 3D microcrack network was then reconstructed and visualized. The key result from the observations is the occurrence of cracks in more or less every resin-rich region [Fig. 4]. The most important cracks seem to be located in surface ply resin-rich regions (135° plies) and interlayer gaps (90° plies). On the whole of observed volume, we found that cracks are mainly oriented along the length of the resin-rich regions, a small number of them however may go through the width of those regions [Fig. 5]. This crack morphology variety can lead to a high scatter in the crack counting by 2D classical observation on the specimen sides [2]. Virtual cuts of the 3D microcrack network may show it well. At the interface between two contiguous plies, the contiguous crack connection goes through the common resin area [Fig. 6]. Delamination was not detected throughout these tests.

5. Conclusion and perspectives

The global resin-rich region geometries were reconstructed and the representative 3D crack network of the quadriaxial reinforced by NC2® subjected to thermal fatigue 400 cycles was revealed. A quantification of resin-rich regions should be carried out so that the real fiber volume fraction outside the disturbance regions would be determined. The spatial location of crack network inside the resin-rich regions should be picked up.
Future fatigue testing will be performed to know how those cracks may propagate with cycle numbers and especially whether they propagate outside the resin-rich regions through the composite plies. The damage criterion would be then taken care.

Acknowledgment

This research would not have been possible and the results achieved would not have been outstanding without the cooperation and the competence of X-ray tomography group at SPIN (Sciences des Processus Industriels et Naturels).

The authors would also like to thank the HEXCEL Company for the material knowledge as well as the original equipment.

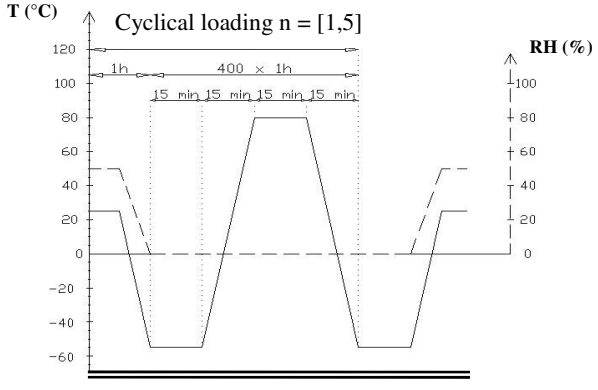

Fig. 1. Cyclical purely thermal loading.

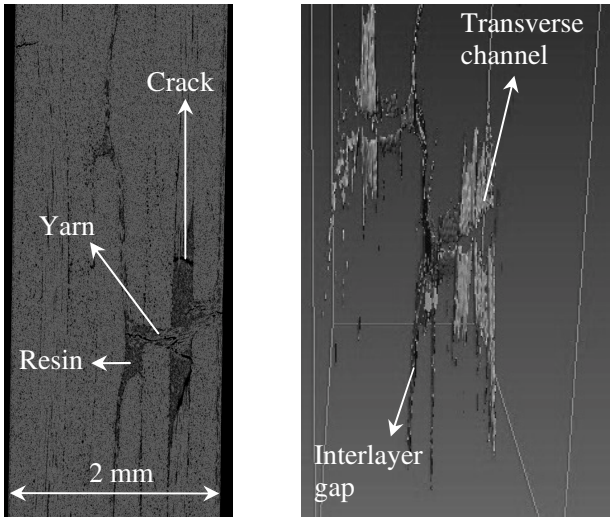

a) b)

Fig. 2. 3D Morphology of a quadriaxial laminate. a) X-ray microtomography reconstructed cross-section. b) Resin-rich regions (stitching yarn section is not presented).

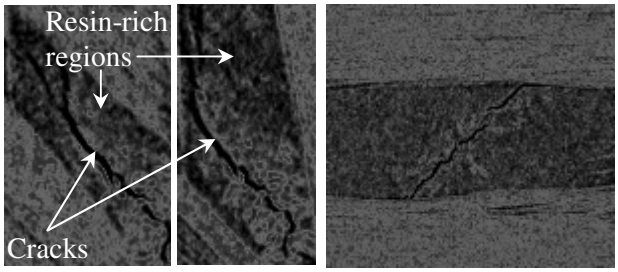

135° Ply 0° Ply 90° Ply

Fig. 6. Crack connection at two contiguous plies interface.

Fig. 5. Crack morphology inside resin-rich region.

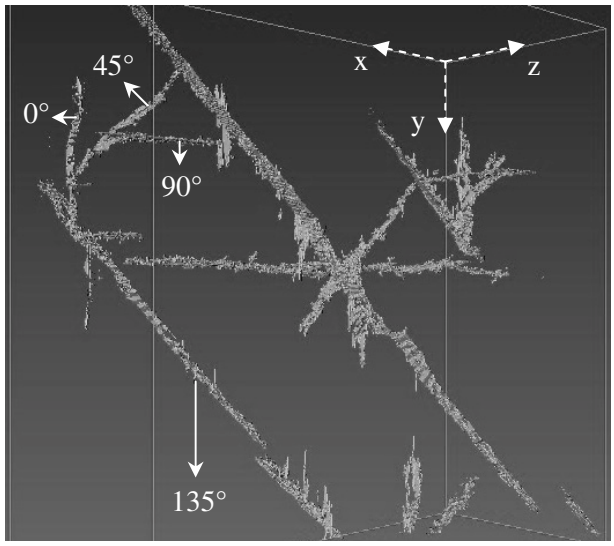

Fig. 4. Microcracking network of a quadriaxial laminate

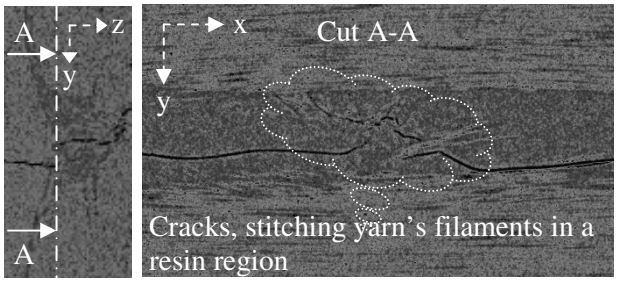

Fig. 3. Cuts from a 3D resin-rich region morphology.

Constituents	Nomenclature	Filement count	Filament Φ (µm)	Twist (t/m)	Density (g/cm3)	Linear density (tex)
Fibre	Toho Tenax HTS 5631	12000	7	0	1.76	0.068
Resin	RTM6	-	-	-	1.14	-
Stitching yarn	PET (Polyester)	24	18	-		7.6

Nomenclature	E (GPa)	ν	σtens ultime (Mpa)	Elongation (%)	CTE (10-6/K)	Service temperatures
Toho Tenax HTS 5631	238/25	0.27/0.028	4300	1.8	-0.1	[, 160°C]
RTM6	2.89	0.38	75	3.4	50	[-60°C, 180°C]
PET (Polyester)	8.4/[2.8, 4.1]		[55, 75]	21	[5, 50]/[40, 100]	[, 163°C]

Tab. 1. Constituent properties of the composite reinforced by NC2® (longitudinal / transversal).

References

[1] PJ. Liotier, A. Vautrin, C. Delisée "Characterization of 3D morphology and microcracks in composites reinforced by multi-axial multi-ply stitched preforms". *Composites: Part A*, 41, pp 653-662, 2010.

[2] PJ. Liotier, A. Vautrin, JM. Béraud "Microcracking of composites reinforced by stitched multiaxials subjected to cyclical hygrothermal loadings". *Composites: Part A*, *In Press*, 2011.

[3] F. Cosmi, A. Bernasconi, N. Sodini "Phase contrast micro-tomography and morphological analysis of a

short carbon fibre reinforced polyamide". *Composites Science and Technology*, 71, pp 23-30, 2011.

[4] A. Bernasconi, F. Cosmi, D. Dreossi "Local anisotropy analysis of injection moulded fibre reinforced polymer composites". *Composites Science and Technology*, 68, pp 2574-2581, 2008.

[5] P. Badel, E. Vidal-Sallé, E. Maire, P. Boisse "Simulation and tomography analysis of textile composite reinforcement deformation at the mesoscopic scale". *Composites Science and Technology*, 68, pp 2433-2440, 2008.

[6] J.S.U. Schell, M. Renggli, G.H. van Lenthe, R. Mu¨ ller, P. Ermanni "Micro-computed tomography determination of glass fibre reinforced polymer meso-structure". *Composites Science and Technology*, 66, pp 2016-2022, 2006.

[7] PJ. Schilling, BR. Karedla, AK. Tatiparthi, MA. Verges, PD. Herrington "X-ray computed microtomography of internal damage in fiber reinforced polymer matrix composites". *Composites Science and Technology*, 65, pp 2071-2078, 2005.

[8] L. Salvo, P. Cloetens, E. Maire, S. Zabler, J.J. Blandin, J.Y. Buffière, W. Ludwig, E. Boller, D. Bellet, C. Josserond "X-ray micro-tomography an attractive characterisation technique in materials science". *NIM B Beam interactions with Materials & Atoms*, 200, pp 273-286, 2003.

[9] Q. Nguyen Thi Thuy, PJ. Liotier, JM. Béraud, A. Vautrin "Microcracking of new composites based on multiaxial multiply stitched performs under cyclical thermal loadings". *JNC 17, Poitiers, France,* pp 1-9, 2011.

[10] D.S. Mikhaluk, T.C. Truong, A.I. Borovkov, S.V. Lomov, I. Verpoest "Experimental observations and finite element modelling of damage initiation and evolution in carbon/epoxy non-crimp fabric composites". *Engineering Fracture Mechanics*, 75, pp 2751-2766, 2008.

[11] S.V. Lomov, E.B. Belov, T. Bischoff, S.B. Ghosh, T. truong chi, I. verpoest "Carbon composites based on multiaxial multiply stitched preforms. Part 1. Geometry of the preform". *Composites: Part A*, 33, pp 1171-1183, 2002.

[12] H. Heb, Y.C. Roth, N. Himmel "Elastic constants estimation of stitched NCF CFRP laminates based on a finite element unit-cell model". *Composites Science and Technology*, 67, pp 1081–1095, 2007.

[13] V. Bellenger, J. Decelle, N. Huet "Ageing of a carbon epoxy composite for aeronautic applications", *Composites: Part B*, 36, pp 189-194, 2000.